On-Line Simultaneous Tuning for Back to Back Converter

R. Tapia Olvera, *Member, IEEE*, O. Aguilar Mejía, *Student Member, IEEE*, J. M. Ramírez Arredondo, *Member, IEEE*, and A. Valderrabano Gonzalez, *Member, IEEE*

Abstract--**This paper presents the simultaneous coordination for back to back control scheme using a B-spline artificial neural network. The main task is that the power converters operation adapt by itself during the grid changes. The basic problem consists of tuning the PI controllers simultaneously when the system and load are subjected to disturbances. The B-spline neural network is an efficient tool to implement the adaptive tuning controllers, with the possibility of carrying out this task on-line taking into account the systems' non-linearities and uncertain situations. The applicability of the proposal is demonstrated by simulation in a back to back configuration connected to a single load. Results show that the proposed controllers' tuning is comparable to that obtained by a conventional design, without requiring a detailed model analysis. The results are analyzed in detail and some important conclusions are drawn.**

Index Terms--**Adaptive control, back to back, power converters, simultaneous tuning.**

I. Introduction

NOWADAYS several applications used power electronics circuits, like electric power converters which transforms the voltage from one type to another (DC-AC or AC-DC). These devices are known as voltage source converters (VSC), where pulse width modulation (PWM) control technique is widely employed. Interfacing circuits deal with power and control stages, using power semiconductor that operate at high frequencies. They become in different topologies and functions for a variety of applications such as motor drives, computer's power adapters, uninterruptible power supplies (UPS), flexible AC transmission systems (FACTS), and alternative energy production systems [1-4].

In the case of electrical power generation wind and solar power may be considered of the most promising renewable energy sources, but the control schemes are an important issue [5]. There are extensive frameworks of various types of electrical machines and controls algorithms that have been developed for wind generator applications [6-10].

Among the schemes of wind energy conversion systems (WECS), the induction machine and permanent magnet synchronous machine are seen as promising elements for energy conversion [6-8,11]. Back to back (BTB) arrangement based on power electronics is required to take advantage of the benefits [12-13]. One of the main tasks that are seeking for the system is that it can operate at variable speed according to the wind nature. However, in order to the electricity can be exploited either in stand-alone operation or connected to the conventional grid, a suitable control scheme is necessary to deal with different operating conditions and uncertainties in the network due to the parameters or load variations.

Several studies that examine wind energy conversion systems have been developed and make different proposals about what should be the control scheme and the tuning methodology [12-16]. [5] presents a review of numerous control strategies adapted for WECS application, thus establishing that there is great interest in getting the best algorithm for secure and reliable system operation. Some of them considered PI controllers for control schemes in back to back converters [17-18]. The linear models design can exhibit some deficiencies for instance the linear controller tuning is guaranteed around an equilibrium point, when the system is subjected to changes in its operating condition or structure the performance is diminished. There are also several proposed adaptive controls to determine the controllers [16, 19-20]. In [20] adaptive PID gains for each controller to achieve satisfactory performance is proposed.

In this paper a B-spline neural network (BSNN) is employed for two main tasks one for PI simultaneous tuning, taking care of a key feature: the proposed controller must be able to enhance the system performance; the second the online parameters updated can be possible. The strategy is proposed to update conventional PI parameters for currently operating in power converters that were tuned time ago. The main idea is to re-tune basically the control gains through an on-line procedure, which involve a few measurements. After that, the same controllers' devices may continue working properly under different operating conditions and topologies. Results show that this idea works adequately, independently of the operation condition.

This work was supported in part by the FOMIX-CONCAYT under Grant 130107 and PROMEP Redes Temáticas de Colaboración.

R. Tapia Olvera and O. Aguilar Mejía are with the Engineering Department, Universidad Politécnica de Tulancingo, Calle Ingenierías 100, Huapalcalco, Hidalgo, México (e-mail: rtapia,[oaguilar]@upt.edu.mx).

J. M. Ramirez Arredondo is with the Electrical Engineering Department, CINVESTAV, Av. del Bosque 1145, colonia el Bajío, Zapopan, 45019, Jalisco, México (e-mail: jramirez@gdl.cinvestav.mx).

A. Valderrabano Gonzalez is with the Engineering Department, Universidad Politécnica de la Zona Metropolitana de Guadalajara, Carretera Tlajomulco Santa Fe k.m. 3.5 No. 595 Col. Lomas de Tejeda Tlajomulco de Zúñiga, Jalisco, México (e-mail: antonio.valderrabano@upjal.edu.mx).

978-1-4673-2673-5/12/$31.00©2012IEEE

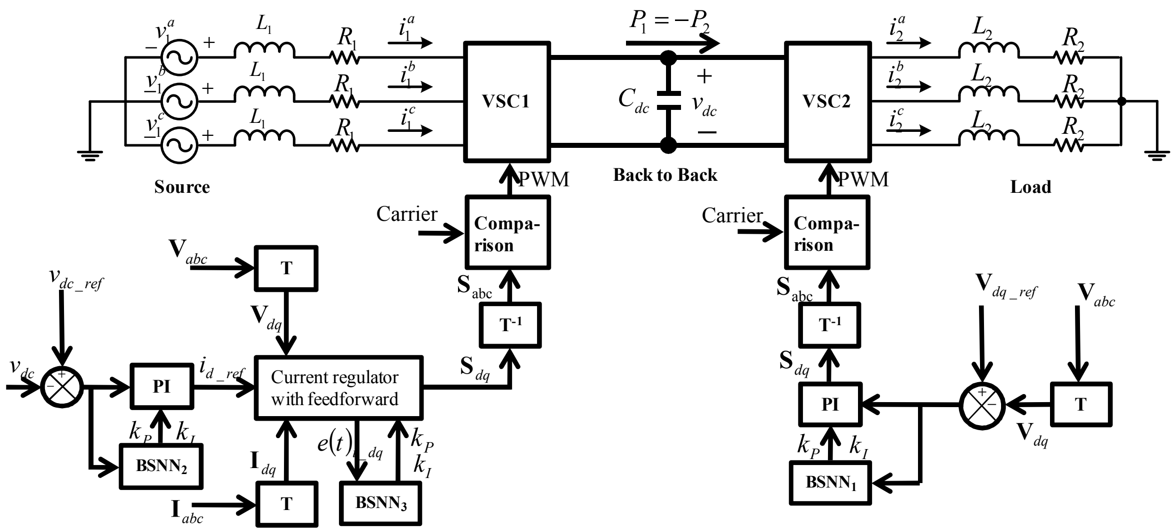

Fig. 1. Back to back converter schematic diagram.

II. AC-DC-AC Converter Model

The back to back converter shown in Fig. 1 is formed by two shared VSC with a common DC bus. Both converters can operate as a rectifier or inverter depending on the power flow direction and the operation is complementary. The source side converter is designated as VSC1 and the converter connected to the load side as VSC2. Assuming a balanced three-phase system without harmonics, phase voltages and currents for the system shown in Fig. 1 are given by,

$$\begin{aligned} v_{1,2}^a &= V_{1,2}\sin\left(\omega_{1,2}t\right) \\ v_{1,2}^b &= V_{1,2}\sin\left(\omega_{1,2}t - \frac{2\pi}{3}\right) \\ v_{1,2}^c &= V_{1,2}\sin\left(\omega_{1,2}t + \frac{2\pi}{3}\right) \end{aligned} \quad (1)$$

$$\begin{aligned} i_{1,2}^a &= I_{1,2}\sin\left(\omega_{1,2}t + \phi_{1,2}\right) \\ i_{1,2}^b &= I_{1,2}\sin\left(\omega_{1,2}t + \phi_{1,2} - \frac{2\pi}{3}\right) \\ i_{1,2}^c &= I_{1,2}\sin\left(\omega_{1,2}t + \phi_{1,2} + \frac{2\pi}{3}\right) \end{aligned} \quad (2)$$

where the voltage and current VSC1 input and VSC2 output are represented by 1,2; $\emptyset_{1,2}$ is the phase angle between voltage and current.

A. VSC Dynamic Model

The VSC shown in Fig. 2 is the three-phase diagram with three-wire connected to the AC load represented by an equivalent Thevenin circuit by means a coupling transformer inductance and resistance (L_T, R_T). The converter DC terminal is connected to a shunt capacitance, C_{dc}, and resistance, R_{dc}, representing the losses of the switching and affiliated components. The three-phase AC side VSC voltage balancing equations are expressed as [21]:

$$L_S\frac{d\mathbf{I}_{abc}}{dt} + R_S\mathbf{I}_{abc} + L_T\frac{d\mathbf{I}_{abc}}{dt} + R_T\mathbf{I}_{abc} = \mathbf{V}_{Sabc} - \mathbf{V}_{Tabc} \quad (3)$$

where $\mathbf{I}_{abc} = [I_a \quad I_b \quad I_c]^T$; $\mathbf{V}_{Sabc} = [V_{Sa} \quad V_{Sb} \quad V_{Sc}]^T$; $\mathbf{V}_{Tabc} = [V_{Ta} \quad V_{Tb} \quad V_{Tc}]^T$ are the three phase current, source and terminal voltage vector, respectively.

The rms amplitude $V_{Tm} = m_0 V_{dc}$ is obtained by the PWM modulation index $(0 < m_0 < 1)$. The frequency ω and phase angle $\emptyset_T$ are PWM voltage source converter controllable variables. When it is connected to a constant frequency load or AC system only V_{Tm} and $\emptyset_T$ need to be used for the control structure.

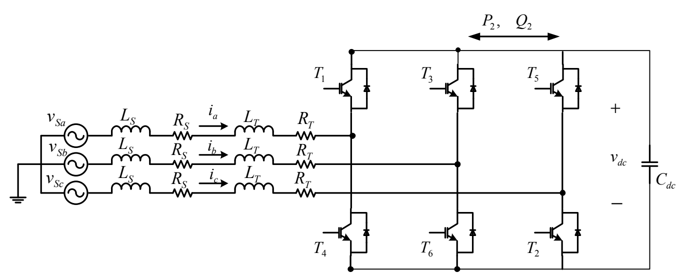

Fig. 2. Voltage source converter model.

The DC-side voltage dynamic expression is deduced based on power balance between the AC and DC-side as,

$$v_{dc}(t)i_{dc}(t) = P(t) - P_L(t) \quad (4)$$

where $P(t)$ is the instantaneous real power at point of common coupling voltage; $P_L(t)$ includes the total power loss; and $P_{dc} = v_{dc}i_{dc}$ is the transferred power from the DC side to the load. Loss components include: a) capacitor dielectric loss, b) switching and on-state loss, and c) losses in the converter AC-side components represented by R_{dc}. The DC current is:

$$C_{dc}\frac{d\,v_{dc}}{dt} = i_{dc} - \frac{v_{dc}}{R_{dc}} \quad (5)$$

and the DC and AC side power balancing:

$$v_{dc}i_{dc} = \mathbf{I}_{\mathbf{abc}}^{T}\mathbf{V}_{\mathbf{Sabc}} - R_S\mathbf{I}_{\mathbf{abc}}^{T}\mathbf{I}_{\mathbf{abc}} - R_T\mathbf{I}_{\mathbf{abc}}^{T}\mathbf{I}_{\mathbf{abc}} - \frac{L_S}{2}\frac{d\left(\mathbf{I}_{\mathbf{abc}}^{T}\mathbf{I}_{\mathbf{abc}}\right)}{dt} - \frac{L_T}{2}\frac{d\left(\mathbf{I}_{\mathbf{abc}}^{T}\mathbf{I}_{\mathbf{abc}}\right)}{dt} \tag{6}$$

B. Control Structure

The control objectives which are set for the BTB operation depend on the application, for instance: 1) AC voltage; 2) AC frequency; 3) active power; 4) reactive power; and 5) DC voltage regulation. Two control tasks are assigned to each VSC and how they allocate can be arbitrary. Fig. 1 shows the BTB converter control structure.

The control targets choice and thus the drivers are depending on the application. For example distributed generation systems it is usual that the control block includes a scheme for regulating the AC frequency and voltage. Therefore, in this paper we are controlled AC voltage and frequency value but also DC link voltage regulation is required.

The VSC2 must ensure constant values for load variables. In this converter the control problem is to determine the reference signal in the PWM control scheme to allow the terminal voltage tracking the desired reference values. The carrier signal is fixed in 2 KHz for 60 Hz load. Hence, the needed measurement is the three-phase voltage at the connection point. For control purpose a dq0 conversion is employed,

$$\mathbf{V}_{dq0} = \mathbf{T}\mathbf{V}_{abc} \tag{7}$$

where,

$$\mathbf{T} = \frac{2}{3}\begin{bmatrix} \sin(\omega t) & \sin\left(\omega t - \frac{2\pi}{3}\right) & \sin\left(\omega t + \frac{2\pi}{3}\right) \\ \cos(\omega t) & \cos\left(\omega t - \frac{2\pi}{3}\right) & \cos\left(\omega t + \frac{2\pi}{3}\right) \\ \frac{1}{2} & \frac{1}{2} & \frac{1}{2} \end{bmatrix} \tag{8}$$

The angular velocity is acquired by PLL strategy and the error signal employed for obtaining the PWM reference signal is, Fig. 1,

$$\mathbf{e}(t) = \begin{bmatrix} v_{d\_ref} \\ v_{q\_ref} \end{bmatrix} - \begin{bmatrix} v_d \\ v_q \end{bmatrix} \tag{9}$$

Defining the voltage as reference, there are two separate axes 90 electrical degrees. d-axis is in phase with the reference vector, whereas-q axis is delayed 90 degrees respect to voltage, similarly, into a d-q component the current is decomposed. Therefore, $v_{d\_ref} = 1.0$ pu and $v_{q\_ref} = 0.0$. For computing the PWM reference signal in dq frame a PI controller is included, after that, an inverse transform is applied from dq to abc. To obtain a PWM signal for VSC2 control a comparison between this signal and the carrier one is done, Fig. 1.

In the case of VSC1 a DC link voltage control is carried out, one possible strategy implied that the reactive power flow must be zero. The regulator scheme needs the voltage and current measurement from the source, similar to VSC2 the dq0 transformation is applied. The first PI controller is required to attain d current reference, i_{d_ref}, based on v_{dc} error signal, i_{q_ref} is fixed equal to zero. The input for the second PI controller is,

$$\mathbf{e}(t) = \begin{bmatrix} i_{d\_ref} \\ i_{q\_ref} \end{bmatrix} - \begin{bmatrix} i_d \\ i_q \end{bmatrix} \tag{10}$$

Current regulator with feedforward voltage and current signals obtains the PWM reference signal in dq frame [22]. Hence, an inverse transform is applied from dq to abc, Fig. 1. The carrier wave is established equal to VSC2.

This paper proposes the use of adaptive PI controllers to maintain the voltage and frequency AC load and DC link voltage constant, Fig. 1. We have three PI controllers that must be tuning to achieve the best back to back converter performance. Reactive power flow should be maintained close to zero. Both parameters the proportional and integer gains are updated online to attain a proper performance under different operating conditions, without restructuring the control scheme.

III. Controller Tuning

The proposed can be achieved adding a B-spline neural network to update k_P and k_I gains in the three PI controllers, Fig. 1, where each PI transfer function is given by,

$$\frac{U(s)}{E(s)} = \frac{k_I + k_p s}{s} \tag{11}$$

Thus, k_P and k_I are updated from a B-spline neural network at every sampled time. With this purpose, six artificial neural networks (ANN) are assembled in the control scheme.

The major advantages of the artificial neural networks are the controller's design simplicity, and their compromise between the complexity of a conventional nonlinear controller and its performance. The B-spline neural networks are a particular case of neural networks that allow to control and model systems adaptively, with the option of carrying out such tasks on-line, and taking into account the power grid non-linearities.

A. Neural network scheme

A B-spline function is a piecewise polynomial mapping, which is formed from a linear combination of basis functions, and the multivariate basis functions are defined on a lattice [23]. The on-line B-spline associative memory network (AMN) adjusts its weights iteratively in an attempt to reproduce a particular function, whereas an off-line or batch B-spline algorithm typically generates the coefficients by matrix inversion or using conjugate gradient. B-spline AMNs adjust their (linear) weight vector, generally using instantaneous least mean square (LMS)-type algorithms, in order to realize a particular mapping, modifying the strength with which a particular basis function contributes to the network output.

Through BSNN there is the possibility to bound the input space by the basis functions definition. Generally, only a fixed number of basis functions participate in the network's output. Therefore, not all the weights have to be calculated each sample time, thus reducing the computational effort and time.

The BSNN's output can be described by [23],

$$y = \mathbf{a}^T\mathbf{w} \tag{12}$$

$$\mathbf{w} = [w_1 \quad w_2 \cdots \quad w_p]^T; \quad \mathbf{a} = [a_1 \quad a_2 \cdots \quad a_p]^T \tag{13}$$

where w_i and a_i are the i-th weight and the i-th BSNN basis function output, respectively; p is the number of weighting factors.

In this paper it is proposed that k_P and k_I be adapted through one B-spline neural network, respectively, for each voltage source converter. The error signals described in section II, e_x, are the inputs to adapt the gains, Fig. 1. Such election is made based on the close relationship between controllers and gains performance. Then the dynamic control parameters for back to back system can be described as follows:

$$K_p = NN_m(e_x, w_m) \tag{14}$$

$$K_I = NN_m(e_x, w_m) \tag{15}$$

where NN_m denotes the B-spline network which is used to calculate K_P and K_I; w_m is the corresponding weighting factor; $m = 1,2,3$ number of PI controllers. Fig. 3 depicts a scheme of the proposed B-spline neural network.

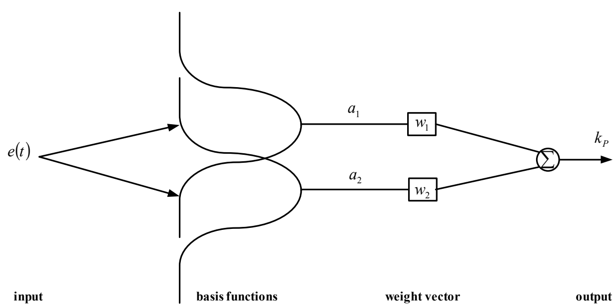

Fig. 3. Proposed BSNN for adapting K_P and K_I control parameters.

The appropriate design requires the following a-priori information: the bounded values of e_x, the size, shape, and overlap definition of the basis function. Such information allows to bound the BSNN input and to enhance the convergence and stability of the instantaneous adaptive rule [23]. Likewise, with this information the BSNN estimates the optimal weights' value. The neural network adaptive parameters, (12)-(15) are created by univariate basis functions of order 3, considering that e_x are bounded within [-12, 12].

B. Learning rule

Learning in artificial neural networks is usually achieved by minimizing the network's error, which is a measure of its performance, and is defined as the difference between the actual output vector of the network and the desired one.

On-line learning of continuous functions, mostly via gradient based methods on a differentiable error measure is one of the most powerful and commonly used approaches to train large layered networks in general [24], and for non-stationary tasks in particular.

In this application, the parameters' quick updating is looked for. While conventional adaptive techniques are suitable to represent objects with slowly changing parameters, they can hardly handle complex systems with multiple operating modes. The instantaneous training rules provide an alternative so that the weights are continually updated and reach the convergence to the optimal values. Also, conventional nets sometimes do not converge, or their training takes too much time [24-25].

In this paper, the neural network is trained on-line using the following error correction instantaneous learning rule [24],

$$w_i(t) = w_i(t-1) + \frac{\eta e_i(t)}{\|\mathbf{a}(t)\|_2^2} a_i(t) \tag{16}$$

where η is the learning rate and $e_i(t)$ is the instantaneous output error.

Respect to the learning rate, it takes as initial value one point within the interval [0, 2] due to stability purposes [23]. This value is adjusted by trial-and-error. If η is set close to 0, the training becomes slow. On the contrary, if this value is large, oscillations may occur. In this application, it settles down in 0.051 for K_P, and 0.0016 for K_I.

It is proposed that during the actualization procedure, a dead band is included to improve the learning rule convergence. The weighting factors are not updated if the error has a value below 0.1%,

$$w_i(t) = \begin{cases} w_i(t-1) + \dfrac{\eta e_i(t)}{\|\mathrm{a}(t)\|_2^2} a_i(t), & \text{if } |e_i| > 0.0001 \\ w_i(t-1), & \text{otherwise} \end{cases} \tag{17}$$

This learning rule has been elected as an alternative to those that use, for instance, Newton's algorithms for updating the weights [24-25] that require Hessian and Jacobian matrix evaluation. Regarding the weights' updating, (16) should be applied for each input-output pair in each sample time; the updating occurs if the error is different from zero. That is the reason because it is said that the weights converge to optimal values [23].

Thus, the proposition consists fundamentally on establishing its structure (the definition of basis functions) and the value of the learning rate. Regarding the weights' updating, (16) should be applied for each input-output pair in each sample time; the updating occurs if the error is different from zero. Respect to the learning rate, it takes as initial point one value inside the interval [0, 2] due to stability purposes. This value is adjusted through trial-and-error; with a value close to zero the training becomes slow.

Hence, the BSNN training process is carried out continuously on-line, while the weights' values are updated using only two feedback variables.

IV. Test Results and Analysis

In order to demonstrate the feasibility of this proposition, a back to back scheme is employed. Matlab-Simulink [26] are used for simulation, the proposed tuning performance is exhibited. To analyze the results, simulations are developed under different scenarios with PI controllers tuned by BSNN (dynamic parameters), ANNPI. Some operating conditions are taken into account. To examine the results three situations are presented. The systems data are: for the source 23KV, 50MVA, 60Hz and the load 60 Hz, 20KW, 380V.

The first condition shows when the system starts its operation, the variables have a zero value. Fig. 4 exhibits the load voltage evolution; about 2 cycles to achieve the stationary state are needed.

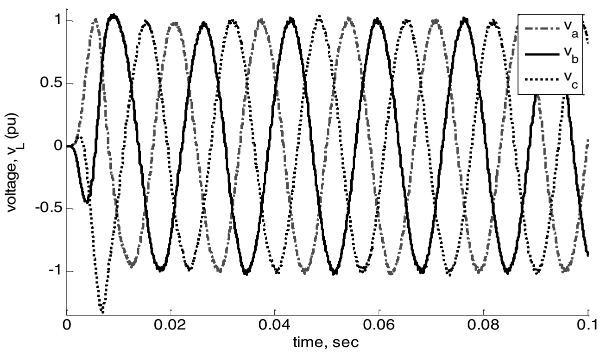

Fig. 4. Load voltage when the operation system starts, *case 1*.

The PWM behavior by terminal voltage converter is observed, Fig. 5 presents the phase a. The PI control parameters obtained by means an adaptive scheme display very well performance, allowing the converters to operate properly and the interest variables reach the desired steady state value. Fig. 6 exemplifies the BSNN performance for k_P gain in controllers 2 and 3; the initial values are 0.3 and 5.4, respectively.

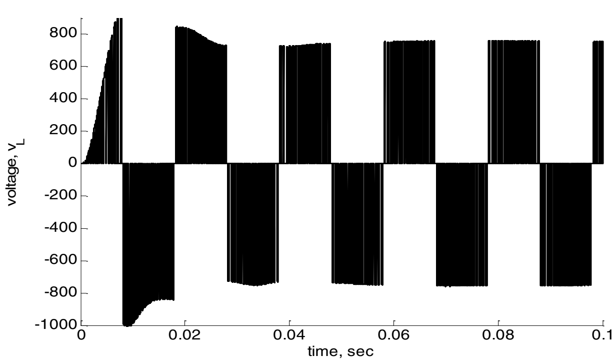

Fig. 5. Converter terminal voltage when the operation system starts, *case 1*.

The second condition illustrates the system's evolution when the load is increased in 100 percent. It is clear the transient response is smaller than the first case due essentially the initial conditions are different to zero. The controllers with adaptive control parameters have a very short transient time, less than one cycle, Fig. 7-9.

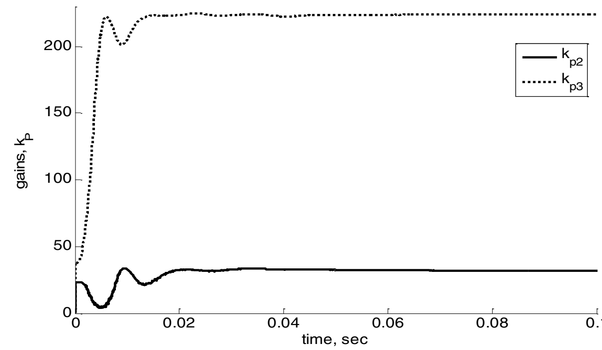

Fig. 6. Proposed BSNN for adapting K_P gains in controllers 2 and 3, c*ase 1*.

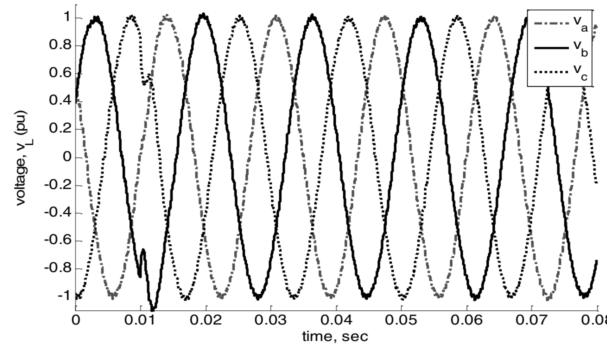

Fig. 7. Load voltage when the load is increased 100 percent, *case 2*.

Fig. 7 presents the load voltage and Fig. 8 the source current. Fig. 9 displays the integral gain's evolution for controller three. Quite similar results are exhibited for all adaptive parameters.

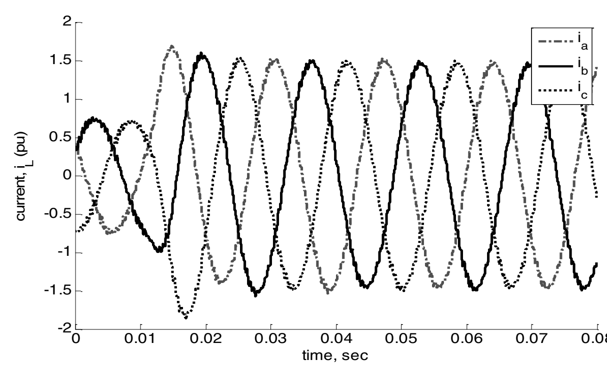

Fig. 8. Source current when the load is increased, *case 2*.

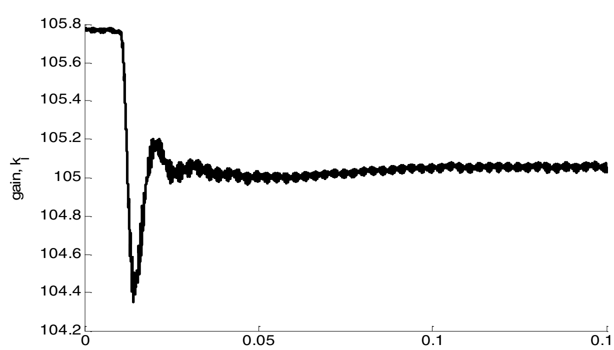

Fig. 9. Proposed BSNN for adapting K_I parameter in controller 3, *case 2*.

The third case validates the appropriate system evolution under load parameters change; phase-to-phase rms voltage is 400V and the frequency is 50Hz. The load and source voltages of phase a, with the new requirements are shown in Fig. 10.

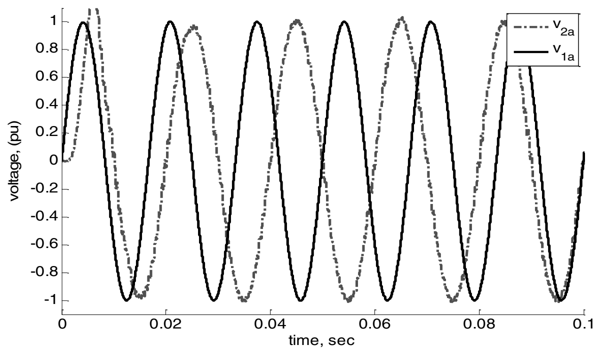

Fig. 10. Load and source voltage at 50 and 60 Hz, respectively, *case 3*.

Fig. 11 exhibits the dynamic behavior of the reactive power at DC link bus, where the proposed scheme is worked. The tuning technique behavior is in accordance with conditions 1 and 2. The ANNPI exhibits very well performance adapting itself to the new conditions. Finally, reactive power exchange between VSC converters is presented in Fig. 12 when the load is increased 200 percent. All variables in the three cases achieve the desired values by means proposed simultaneous tuning technique.

The steady-state parameters reached by the neural network for PI design, shown that they are updated under different operating conditions. Thus, depending on the system topology, these parameters modify their value. In this case the steady state values are $k_P = [760.2358 \quad 32.0549 \quad 223.3065]$ and $k_I = [549.4560 \quad 19.4280 \quad 105.0667]$.

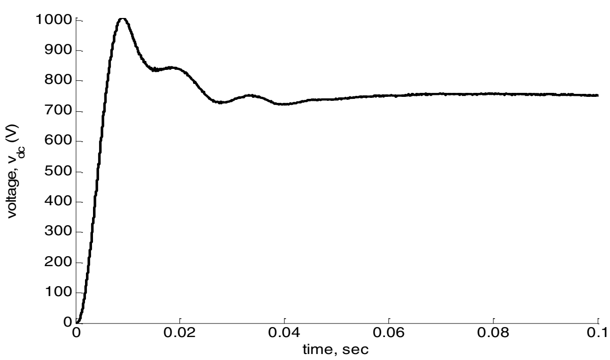

Fig. 11. DC link voltage performance, *case 3*.

V. Conclusions

The aim of the paper is to show the performance of adaptive PI parameters as a mean to tune linear controllers in back to back structure. In order to attain such purposes a B-spline neural network-based is proposed. With this neural adaptive scheme, the possibility to implement the on-line updating parameters is potential due to it has learning ability and adaptability, robustness, simple algorithm and fast calculations, and not exclusive but inclusive, nature to get better solution under hardware's constraints. This is desirable for practical hardware implementation in power stations.

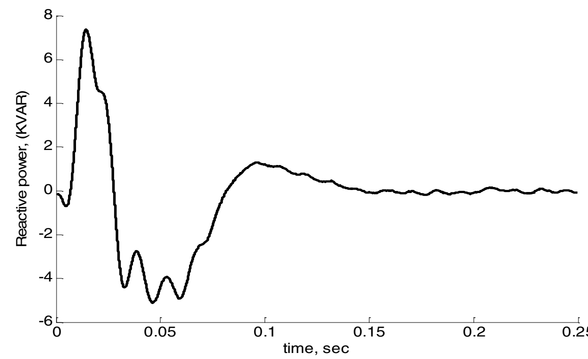

Fig. 12. Reactive power exchange when the load is increased 200 percent.

Unlike the conventional technique, the B-spline NN exhibits an adaptive behavior since the weights can be adapted on-line responding to inputs and error values as they arise. Also, it can take into account nonlinearities, un-modeled dynamics, and un-measurable noise. Simulations on back to back structure under different disturbances and operating conditions, demonstrate the effectiveness and robustness of the proposed strategy. Dynamic and steady state response are analyzed.

VI. References

[1] Narain G. Hingorani, Laszlo Gyugyi, *Understanding FACTS*, IEEE Press Editorial Board, 2000.

[2] R. Dávalos, J. M. Ramírez, and R. Tapia, "Three-phase multi-pulse converter StatCom analysis", *International Journal of Electrical Power & Energy Systems*, vol. 27, pp. 39–51, 2005.

[3] R. Sternberger, and D. Jovcic, "Theoretical Framework for Minimizing Converter Losses and Harmonics in a Multilevel STATCOM" *IEEE Trans. Power Delivery*, vol. 23, No. 4, pp. 2376- 2384, 2008.

[4] Yi Wang, Lie Xu, "Coordinated Control of DFIG and FSIG-Based Wind Farms Under Unbalanced Grid Conditions", *IEEE Trans. Power Delivery*, vol. 25, No. 1, pp. 367-377, January 2010.

[5] Hoa M. Nguyen, D. Subbaram Naidu, "Advanced Control Strategies for Wind Energy Systems: An Overview", 2011 IEEE PES Power Systems Conference & Exposition (PSCE).

[6] G.O. Cimuca, C. Saudemont, B. Robyns, and M.M. Radulescu, "Control and performance evaluation of a flywheel energy-storage system associated to a variable-speed wind generator," *IEEE Trans. Industrial Electronics*, vol. 53, No. 4, pp. 1074-1085, 2006.

[7] S. Niu, K.T. Chau, J.Z. Jiang, and C. Liu, "Design and control of a new double-stator cup-rotor permanent-magnet machine for wind power generation," *IEEE Trans. Magnetics*, vol. 43, No. 6, pp. 2501-2503, 2007.

[8] C. Yu, K.T. Chau and J. Z. Jiang, "A flux-mnemonic permanent magnet brushless machine for wind power generation," *Journal of Applied Physics*, vol. 105, No. 7, pp.1-3, 2009.

[9] D.A. Torrey, "Switched reluctance generators and their control," *IEEE Trans. Industrial Electronics*, vol. 49, No. 1, pp. 3-14, 2002.

[10] F. Valenciaga and P.F. Puleston, "Supervisor control for a stand-alone hybrid generation system using wind and photovoltaic energy," *IEEE Trans. Energy Conversion*, vol. 20, No.2, pp. 398-405, 2005.

[11] P. B. Eriksen, T. Ackermann, H. Abildgaard, P. Smith, W. Winter, and J. M. Rodriguez Garcia, "System operation with high wind penetration," *IEEE Power Energy Mag*, vol. 3, no. 6, pp. 65–74, 2005.

[12] S. Mishra, Y. Mishra, Fangxing Li, Z. Y. Dong, "TS-fuzzy controlled DFIG based Wind Energy Conversion Systems", *IEEE Power & Energy Society General Meeting*, pp. 1-7, 2009.

[13] F. M. Hughes, O. Anaya-Lara, N. Jenkins, and G. Strbac, "Control of DFIG-based wind generation for power network support," *IEEE Trans. Power Systems*, vol. 20, No. 4, pp. 1958–1966, 2005.

[14] Van-Tung Phan, Hong-Hee Lee, "Performance Enhancement of Stand-Alone DFIG Systems With Control of Rotor and Load Side Converters Using Resonant Controllers", *IEEE Trans. Industry Applications*, vol. 48, No. 1, 2012.

[15] J. Hu, H. Nian, B. Hu, Y. He, and Z. Q. Zhu, "Direct active and reactive power regulation of DFIG using sliding-mode control approach," *IEEE Trans. Energy Convers*., vol. 25, No. 4, pp. 1028–1039, 2010.

[16] Mostafa Soliman, O. P. Malik, David T. Westwick, "Multiple Model Predictive Control for Wind Turbines With Doubly Fed Induction Generators", IEEE Trans. Sustainable Energy, vol. 2, No. 3, 2011.

[17] H. Camblong, I. M. de Alegria, M. Rodriguez, and G. Abad, "Experimental evaluation of wind turbines maximum power point tracking controllers," *Energy Convers. Manage*., vol. 47, pp. 2846–2858, 2006.

[18] A. D. Hansen, P. Sorensen, F. Lov, and F. Blaabjerg, "Control of variable speed wind turbines with doubly-fed induction generators," Wind Eng., vol. 28, pp. 411–443, 2004.

[19] E. B. Muhando, T. Senjyu, A. Yona, H. Kinjo, and T. Funabashi, "Disturbance rejection by dual pitch control and self-tuning regulator for wind turbine generator parametric uncertainty compensation," *IET Control Theory Applicat*., vol. 1, pp. 1431–1440, 2007.

[20] M. Sedighizadeh, D. Arzaghi-Harris, and M. Kalantar, "Adaptive PID control of wind energy conversion systems using RASP1 mother wavelet basis function networks," IEEE Conference in TENCON, vol. C, pp. 524 – 527, Nov. 2004.

[21] J. Arrillaga, Y. Liu, N. Watson and N. Murray, Self-Commutating Converters for High Power Applications. United Kingdom: Wiley, 2009.

[22] Z. Zhou, P.J. Unsworth, P.M. Holland, P. Igic, "Design and analysis of a feedforward control scheme for a three-phase voltage source pulse width modulation rectifier using sensorless load current signal", IET Power Electron., vol. 2, No. 4, pp. 421–430, 2009.

[23] Brown, and C. Harris, "Neurofuzzy Adaptive Modelling and Control," Prentice Hall International, 1994.

[24] David Saad, "On-line learning in neural networks," Cambridge University Press 1998.

[25] Osman, A. H., Abdelazim, Tamer, and Malik, O. P., Transmission Line Distance Relaying Using on-line Trained Neural Network. *IEEE Trans. Power Delivery*, vol. 20, No. 2, pp. 1257-1264, 2005.

[26] Sybille, G., Brunelle, P., Hoang Le-Huy, Dessaint, L.A., Al-Haddad, K, "Theory and applications of power system blockset, a MATLAB/Simulink-based simulation tool for power systems", *IEEE Power Engineering Society Winter Meeting*, vol. 1, pp. 774-779, 2000.

VII. Biographies

R. Tapia Olvera obtained his BS in Electrical Engineering from Instituto Tecnológico de Pachuca, México in 1999; M.Sc., and Ph. D., in Electrical Engineering from CINVESTAV Guadalajara, México in 2002 and 2006, respectively. He is currently full time professor of Universidad Politécnica de Tulancingo. His primary area of interest is in modeling and control of FACTS devices with computational intelligence techniques.

O. Aguilar Mejia obtained his BS in Electrical Engineering from Instituto Tecnológico de Pachuca, México in 1999; M.Sc. in Electrical Engineering from CINVESTAV Guadalajara, México in 2002. He is currently full time professor of Universidad Politécnica de Tulancingo. His primary area of interest is in modeling and control of electric machinery and automatic control systems.

J. M. Ramirez Arredondo obtained his BS in Electrical Engineering from Universidad de Guanajuato, México in 1984; M.Sc. in Electrical Engineering from UNAM in 1987; the Ph. D. in Electrical Engineering from UANL in 1992. He joined the department of Electrical Engineering of CINVESTAV in 1999, where he is currently a full time professor. His areas of interest are in FACTS devices and control of electrical power systems.

A. Valderrabano Gonzalez obtained his M.Sc. in Electronics Engineering from INAOE, México; Ph. D., in Electrical Engineering from CINVESTAV Guadalajara, México. He is currently full time professor of Universidad Politécnica de la Zona Metropolitana de Guadalajara. His primary area of interest is in modeling and control of power converters.